PCCP

Accepted Manuscript

ROYAL SOCIETY
OF CHEMISTRY

www.rsc.org/pccp

The cluster-assembled nanowires based on $M_{12}N_{12}$ (M=Al and Ga) clusters as potential gas sensors for CO, NO, and NO_2 detection

Yongliang Yong, [a,b*] Huai Jiang,[a] Xiaohong Li,[a] Shijie Lv[a] and Jingxiao Cao[a]

[a]College of Physics and Engineering, Henan University of Science and Technology, Luoyang 471003, People's Republic of China

[b]Department of Physics, Zhejiang University, Hangzhou 310027, People's Republic of China

Abstract: The advance of cluster-assembled materials where clusters serve as building blocks has opened new opportunities to develop ever more sensitive gas sensors. Here using density functional theory calculations, the structural and electronic properties and the applications as gas sensors of cluster-assembled nanowires based on $M_{12}N_{12}$ (M=Al and Ga) clusters have been investigated. Our results show that the nanowires can be produced via the coalescence of stable $M_{12}N_{12}$ fullerene-like clusters. The $M_{12}N_{12}$-based nanowires have semiconducting electrical properties with direct energy gaps, and are particularly stable at room temperature for long enough to allow for their characterization and applications. Further, we found that the CO, NO, and NO_2 molecules are chemisorbed on the $M_{12}N_{12}$-based nanowires with reasonable adsorption energies and apparent charge transfer. The electronic properties of the $M_{12}N_{12}$-based nanowires present dramatic changes after the adsorption of the CO, NO, and NO_2 molecules, especially their electric conductivity.

[*]Corresponding author. Tel: +86 187 36385204

E-mail address: ylyong@haust.edu.cn (Y. Yong)

However, the adsorption of NO_2 on the $Al_{12}N_{12}$-based nanowire is too strong, indicating an impractical recovery time as NO_2 sensors. In addition to this, due to the reasonable adsorption energies, apparent charge transfer, the change of the electric conductivity, and the short recovery time, the $Al_{12}N_{12}$-based nanowire should be good CO and NO sensors with quick response as well as short recovery time, while the $Ga_{12}N_{12}$-based nanowire should be promising gas sensors for CO, NO, and NO_2 detection.

Keywords: gas sensor, cluster-assembled nanowires, $M_{12}N_{12}$ (M=Al and Ga) clusters, DFT calculations.

1. Introduction

Gas sensors have gained in importance in the recent years for applications that include homeland security, space exploration, control of chemical processes, medical and environmental monitoring [1-4]. Accordingly intense research is underway to develop new gas sensing materials and devices. Nanowires have been regarded as one of the most exciting materials for developing new sensing materials and devices, since they offer many advantages such as high surface-to-volume ratios, Debye lengths comparable to the target molecule, low power consumption, and small dimensions [5, 6]. Most nanowire-based gas sensors have applied semiconductors as the sensing materials due to their additional advantages such as low cost, long duration, high sensitivity, and reliability, *etc*. To date, related research has mainly concentrated on

semiconducting metal-oxide nanowires such as ZnO, TiO_2, CuO, and SnO_2 [7-9].

As the archetype of semiconducting nanowires, Group-III nitrides nanowires have been envisioned as nanoscale materials for next-generation technology [10-16] because of their special growth modes and unique 1D structure. In particular, they have been investigated as sensing materials for the detection of different gases [16, 17]. Despite group-III nitrides MN nanowires can be fabricated by a wide range of methods, such as laser ablation, metal-organic vapour phase epitaxy, chemical beam epitaxy, and molecular beam epitaxy (see ref. 11, and references therein), high-quality MN nanowires with small dimension size still remain difficult to produce. It is known that the smaller the diameter of a nanowire is, the higher the surface-to-volume ratio is and the more obvious quantum confinement (mainly the quantum size effect) becomes, making the electrical properties of the nanowire significantly more sensitive to the specific gas molecules adsorbed selectively on the surface [6].

Cluster-assembled materials, which use stable size-specific clusters as building blocks, allow the physical and chemical properties of clusters to be incorporated into designer materials with tailored properties, and thus would exhibit properties very different from materials composed of individual atoms [18-23]. In this context, it is reasonable to expect that the nanowires based on stable MN clusters have unusual properties, which would be quite different from that in the atomic solid phase. Group-III nitrides MN clusters have been extensively investigated and found that $M_{12}N_{12}$ clusters can be viewed as ideal building blocks for the synthesis of cluster-assembled materials [24-30]. For example, Yong *et al.* [29] have reported the

3

results of density functional theory calculations on cluster-assembled materials based on $M_{12}N_{12}$ (M=Al and Ga) fullerene-like clusters. They found that the $M_{12}N_{12}$ clusters can bind into stable assemblies by either six isolated four-membered rings or eight six-membered rings face coalescence, which enables the construction of rhombohedral or cubic nanoporous framework of varying porosity. Then, Liu *et al.* [26] reported a new family of $M_{12}N_{12}$ (M=Al and Ga) cluster-assembled low-density materials with distinguished structures and properties based on state-of-the-art first-principles calculations. Furthermore, recent results have presented a great potential of group-III nitrides MN clusters for application as gas sensors for various toxic gases detection [31-37]. Therefore, it is very interesting and important to study the feasibility of using the nanowires based on stable MN clusters as gas sensors.

It is well known that carbon monoxide (CO) and nitrogen dioxide including NO and NO_2 are one of the most prominent toxic gases in air pollution and for human life. Since gases of interest even at very low concentrations can impact significantly on the surrounding environment, therefore, the capability to detect extremely low levels of these species becomes important. For example, the U.S. Environmental Protection Agency (EPA) recommends an ambient air quality of 9 ppm CO or lower averaged over 8 h and 35 ppm or lower over 1 h. Therefore, in this article, using density functional theory (DFT) calculations, we study the structural stabilities and electronic properties of the $M_{12}N_{12}$-based nanowires (M=Al and Ga) and the adsorption behaviors and electronic properties of CO, NO, and NO_2 on $M_{12}N_{12}$-based nanowires (M= Al and Ga), thus exploring the feasibility of using $M_{12}N_{12}$-based nanowires as

gas sensors. Our results indicate that CO, NO, and NO_2 molecules prefer to chemically adsorb on the $M_{12}N_{12}$-based nanowires with reasonable adsorption energies and apparent charge transfer between nanowire and molecule. The band structures are modified apparently after the three molecules adsorption, indicating that the adsorption of the three molecules changes the electronic properties of the $M_{12}N_{12}$-based nanowires. Accordingly and in view of the recovery time, the $Al_{12}N_{12}$-based nanowire can be used as reusable sensors for CO and NO molecules, while the $Ga_{12}N_{12}$-based nanowire should be promising gas sensors for CO, NO, and NO_2 detection.

2. Computational methods

In this work, all calculations are performed using the spin-polarized density functional theory (DFT) implemented in the DMOL^3 program (Accelyrs Inc.) [38, 39]. The generalized gradient approximation formulated by Perdew, Burke, and Ernzerhof (PBE) [40] is chosen to describe the exchange-correlation energy functional. The double numerical basis sets supplemented with d polarization functions (the DNP sets) and all-electron core treatment are selected. In the self-consistent field calculations, the convergence criterion is set to 10^{-6} a.u. on the energy and electron density. The geometries are fully optimized without any symmetry constraints. The convergence criterion of 10^{-3} a.u. on the gradient and displacement and 10^{-5} a.u. on the total energy in geometrical optimization are used. The periodic boundary condition is employed with a tetragonal supercell of $15 \times 15 \times L$ Å, where L is the length of translational periodicity. The Brillouin zone is sampled by $1 \times 1 \times 5$ special k-points for

using the Monkhorst-Pack scheme [41].

The binding energy per MN (E_b) is defined as $E_b=(nE_M+ nE_N-E_{MN})/n$, where E_M (M= Al and Ga) and E_N are the total energies of an isolated M and N atom, respectively, E_{MN} is the total energy of the corresponding MN system, and n is the number of M or N atoms involved. To investigate the stability of the adsorption of molecules on $M_{12}N_{12}$-based nanowires, the adsorption energy (Eads) is defined as $E_b=E_{(nanowire+molecule)}-E_{(nanowire)}-E_{(molecule)}$, where $E_{(nanowire+molecule)}$, $E_{(nanowire)}$ and $E_{(molecule)}$ is the total energy of the system of molecule adsorbed on nanowire, the corresponding pure nanowire and molecule, respectively. In such a definition, negative adsorption energy indicates that the adsorption is exothermic. The charge transfer between $M_{12}N_{12}$–based nanowire and absorbed molecules is analyzed based on Hirshfeld analysis, which is based directly on the electron density as a function of space. In order to investigate the electronic properties, the DFT calculations are performed on band structures and density of states (DOS) using a $1\times1\times15$ Monkhorst-Pack grid. The accuracy of the GGA-PBE and DNP combination for investigating the structures and electronic properties of MN systems has been confirmed by previous studies (for example, ref. 24).

3. Results and discussion

3.1 The structural and electronic properties of $M_{12}N_{12}$-based nanowires

It is well known that the $M_{12}N_{12}$ (M=Al and Ga) clusters, as shown in Fig.1a, are highly stable with a fullerene-like cage structure with six isolated four-membered rings (4MRs) and eight six-membered rings (6MRs), and possess a high symmetry

6

(Th). We have investigated the formation of $M_{12}N_{12}$ (M=Al and Ga) dimers and their implications for forming framework materials, and found that there are two isomers of $M_{12}N_{12}$ (M=Al and Ga) dimers are relatively stable [24]. The most energetically favorable structure is generated by coalescing two 6MRs of two $M_{12}N_{12}$ monomers dimers to form a double six-membered ring, and in which a 6MR of one monomer is connected with a 4MR of the other monomer (see Fig.1b, denoted as structure A). The 4MRs face coalescence is the second energetically favorable (see Fig.1d, denoted as structure C). However, Liu *et al.* found that the second stable dimer has a new way of coalescence, which adopts a 6MR facing 6MR link and a 6MR of one monomer is connected with a 6MR of the other monomer (see Fig.1c, denoted as structure B) [26]. This is very similar to the cases of the $Zn_{12}O_{12}$ [42, 43] and $Zn_{12}S_{12}$ [44] dimers. The second stable one is only 0.015 eV and 0.019 eV higher in energy for $Al_{12}N_{12}$ and $Ga_{12}N_{12}$, respectively, indicating that these two 6MR face coalescences can be viewed as the ground state of $M_{12}N_{12}$ (M= Al and Ga) dimers.

The relative stability of $M_{12}N_{12}$ (M = Al, Ga) dimers is analyzed by calculating the binding energy per MN (E_b) and dimerization energy (E_d), which is defined as $E_d=2E_{monmer}-E_{dimer}$, where E_{monmer} and E_{dimer} is the total energy of the $M_{12}N_{12}$ monomer and dimer, respectively, which are listed in Table 1. Meanwhile, the HOMO-LUMO gaps are also listed in Table 1. It is found that the E_b of the dimers is larger than the corresponding monomers, indicating that the dimers are more stable than monomers. The E_d of the most stable configuration of is $Al_{12}N_{12}$-based (or $Ga_{12}N_{12}$-based) dimer is up to 8.814 eV (or 6.988 eV), further indicating the stability

of the dimers. In the present work, our DFT-GGA optimization calculations concur with the previous result [26]. The previous studies have predicted that the cluster-assembled materials can be constructed with $M_{12}N_{12}$ (M=Al and Ga) clusters via the 6MR or 4MR face coalescence [24-26]. Therefore, we then discuss the nanowire system constructed with $M_{12}N_{12}$ (M=Al and Ga) clusters.

Since the three stable $M_{12}N_{12}$ dimers have very good axial symmetry features and stable structures, the $M_{12}N_{12}$-based nanowires can be formed by translational symmetry arrangement. The segments of the optimized configurations of $M_{12}N_{12}$-based nanowires are shown in Fig. 1(e-g), and the calculated results are summarized in Table 2. It is found that the structural geometry of the $M_{12}N_{12}$ cluster can be preserved in the assembled nanowires, which is different from the case of B_nN_n clusters [29]. To study the stability of $M_{12}N_{12}$-based nanowires, we calculated their binding energies per MN (E_b). It is found that the E_b of the three nanowires are larger than those of the corresponding dimers and monomers, indicating that the nanowires are more stable than their corresponding dimers and monomers. These features are also found in other semiconductor cluster-assembled materials [24-28, 42-44].

We also calculated the electronic energy band structures of the $M_{12}N_{12}$-based nanowires. The energy bands near the Fermi surface are shown in Fig. 2. The band structures clearly show that the $M_{12}N_{12}$-based nanowires have semiconducting electrical properties with direct energy gaps. The band-gap widths of the $M_{12}N_{12}$-based nanowires listed in Table 2 are much smaller than that of the corresponding nanowires [45, 46] with wurtzite structure, in which the dominate

structural motif can be built up by cutting from the bulk phases, indicating that the electronic properties of $M_{12}N_{12}$-based nanowires are different from that of the corresponding nanowires with wurtzite structure.

To investigate the feasibility of using the $M_{12}N_{12}$-based nanowires as gas sensors, the premise may be that whether they are stable enough in an experimental environment to allow for their characterization and applications. Therefore, to explore the dynamic behavior and thermal stability of the $M_{12}N_{12}$-based nanowires, the first-principles Born-Oppenheimer molecular dynamics (BOMD) simulation within a NVT ensemble was carried out for the most stable structures, namely the nanowire-I as shown in Fig. 1e. A Nosé-Hoover chain of thermostats is used to control the temperature. The GGA-PBE and DNP combination is used here for BOMD. We set a simulation time of 5 ps with a time step of 1fs, and the trajectories were calculated at a constant average temperature of 300 K. Fig. 3 shows how the energies of the structure vary during the simulation. After 5 ps, we found no structure destruction of the $M_{12}N_{12}$-based nanowires. Further, it is observed form Fig. 3 that the energy of the $M_{12}N_{12}$-based nanowires oscillates around the same energy value for the duration of the simulation, a fact that is very supportive of the thermal stability of the calculated structure. Therefore, these results, coupled with the facts of binding energy, demonstrate that the structures of $M_{12}N_{12}$-based nanowires are particularly stable at room temperature for long enough to allow for their characterization and applications.

3.2 The adsorption of CO, NO and NO_2 molecules on the $M_{12}N_{12}$-based nanowires

Since the most stable configuration of $M_{12}N_{12}$-based nanowire is thermally stable

at 300 K, we then investigate the feasibility of the most stable $M_{12}N_{12}$-based nanowire

as a gas sensor material. In order to obtain the most stable configurations of each

molecule adsorbed on $M_{12}N_{12}$-based nanowires, we have set up a lot of initial

structures of the molecule-nanowire systems. For example, the adsorption of CO

molecule on $Al_{12}N_{12}$-based nanowires, we put the CO molecule on the sites of

$Al_{12}N_{12}$-based nanowires, which contains the top of Al or N atom, the center of Al-N

bonds, and the surface of 4MR or 6MR. More importantly, the atom, bonds and

surface in the nanowire are all considered. Meanwhile, we consider the orientation of

CO molecule to the site, for example, the C (or O) of CO molecule points to the top of

Al or N atoms, the CO molecule is parallel or vertical to the Al-N bonds or the surface

of 4MR or 6MR. The most stable and some low-lying structures of the CO, NO, and

NO_2 molecules on the $M_{12}N_{12}$-based nanowires are shown in Fig. 4 and 5, and the

summarized results are listed in Table 3 and 4, respectively. It is noted that only the

molecule adsorption on around the sites of the $M_{12}N_{12}$-based nanowires are shown in

figures, and isometric structures of molecule (CO, NO, and NO_2) adsorbed on the

$M_{12}N_{12}$-based nanowire (M=Al and Ga) are labeled as M-molecule-x (x=1, 2, 3) in

order of decreasing stability.

Then we investigate the adsorption of the CO molecule on the $Al_{12}N_{12}$-based

nanowire. After full relaxation of all possible initial geometries, the CO molecule

adopts the orientation of C atom pointing to the nanowire, and the configuration of

CO located on the top of Al atoms is the most stable, as shown in Fig. 4a, which is

similar to the case of CO molecule adsorption on other clusters [32, 47, 48] and doped

nanotubes [49]. At this configuration the adsorption energy is -0.584 eV, and the distance between CO and nanowire is 2.15 Å, accompanied with a charge transfer of 0.193 e from the CO molecule to the $Al_{12}N_{12}$-based nanowire. This is consistent with the case of CO molecule adsorbed on $Al_{12}N_{12}$ cluster [32]. In the second most stable configuration of CO molecule on the $Al_{12}N_{12}$-based nanowire, one Al-N bond is broken after the CO adsorption, and then the C atom in CO molecule is attached to the Al and O atom. It has an adsorption energy of -0.27 eV, much higher 0.314 eV than the most stable one.

Differing from the case of CO molecule adsorbed on the $Al_{12}N_{12}$-based nanowire, NO is attached to the $Al_{12}N_{12}$-based nanowire with the N-O bond in NO parallel to one Al-N bond, and the N atom in NO attached to the N atom in nanowire while the O atom in NO attached to the Al atom (see Fig. 4c), resulting in an exothermic adsorption energy of -0.720 eV. There is a charge transfer of 0.305 e from the nanowire to the NO molecule. We also obtained the second stable configuration of NO molecule adsorbed on the $Al_{12}N_{12}$-based nanowire as shown in Fig. 4d, which is similar to the case of the most stable structure of CO molecule adsorbed on the $Al_{12}N_{12}$-based nanowire. It has an adsorption energy of -0.648 eV, which is a little higher 0.072 eV than the most stable one. Further, the charge transfer between the nanowire and the NO molecule is small (0.050 e) but obvious. It should be noted that the Hirshfeld scheme gives much smaller atomic charges than nearly all other charge schemes [50].

For the NO_2 molecule adsorption on the $Al_{12}N_{12}$-based nanowire, it is found that

the NO$_2$ molecule is adopted the orientation of O-N-O parallel to one edge of Al-N-Al

in nanowire, and the configuration of NO$_2$ molecule located on this edge is the most

stable, as shown in Fig. 4e. Its adsorption energy is -1.157 eV and there is a charge

transfer of 0.512 e from the nanowire to the NO$_2$ molecule. However, for the second

stable configuration, one O atom of NO$_2$ molecule is attached to one Al atom with the

Al-O distance of 1.92 Å, leading to an adsorption energy of -0.995 eV.

For the CO molecule adsorbed on the Ga$_{12}$N$_{12}$-based nanowire, the most stable

structure is similar to the second stable configuration of CO molecule adsorbed on the

Al$_{12}$N$_{12}$-based nanowire (see Fig. 5a). Its adsorption energy is -0.796 eV, and the

charge transfer between the nanowire and the CO molecule is 0.213 e. When the CO

molecule is located on the junction of Ga$_{12}$N$_{12}$ units, the C atom would be attached to

one N atom and one Ga atom in the other Ga$_{12}$N$_{12}$ unit (see Fig. 5b), leading to an

adsorption energy of -0.457 eV, higher 0.339 eV than that of the most stable one.

Further, we find that the third stable configuration is similar to the most stable case of

CO molecule adsorbed on the Al$_{12}$N$_{12}$-based nanowire, and its adsorption energy is

-0.327 eV, which is much higher 0.469 eV than the corresponding most stable one.

Although we have considered as possible as many initial structures of NO

molecule on Ga$_{12}$N$_{12}$-based nanowire, it is found that, after full relaxation, there is one

chemically adsorbed configuration of NO molecule on the Ga$_{12}$N$_{12}$-based nanowire as

shown in Fig. 5d, which is similar to the second stable case of NO molecule adsorbed

on the Al$_{12}$N$_{12}$-based nanowire. At this configuration the adsorption energy is -0.405

eV, and the molecule-nanowire distance is 2.29 Å, accompanied with small charge

transfer (0.053 e) from the molecule to nanowire.

Very different from the adsorption of NO_2 on the $Al_{12}N_{12}$-based nanowire, the NO_2 molecule shows strong interaction with the nanowire when one O atom of NO_2 molecule points to a Ga atom (see Fig. 5e), result in exothermic adsorption energy of -0.675 eV and the formation of Ga-O bond (bond length is 2.04 Å). When the N atom of NO_2 points to a Ga atom, it forms the second stable configuration with adsorption energy of –0.399 eV and the nanowire-molecule distance of 2.16 Å. From Table 4, it can be seen that there is a charge transfer of at least 0.14 e between the nanowire and the NO_2 molecule after the NO_2 molecule.

Since materials exhibiting magnetic properties are in great demand for applications in nanoscale electronics and spintronics, we have investigated the magnetic properties of the molecule-nanowire systems. The spin states of these systems are shown in Fig. 6. It is known that the pure $M_{12}N_{12}$-based nanowires are nonmagnetic. The adsorption of NO and NO_2 molecules introduces spin polarization into the $M_{12}N_{12}$-based nanowires with magnetic moment of approximately 1 μ_B. That is to say, the net spin polarization of the $M_{12}N_{12}$-based nanowires is drastically modified by about 1 μ_B after the adsorption of NO (or NO_2) molecule, indicating that it can be exploited as a highly sensitive novel gas detection technique based on the measurement of local magnetic moment in the $M_{12}N_{12}$-based nanowires using various experimental technique such as magnetic AFM or SQUID magnetometer [51]. We also calculated the magnetic moment on each atom in the systems to further investigate the origin and distribution of the magnetic moment. The spin densities of

13

some representative systems are shown in Fig. 6. The magnetic moment is mainly located on the molecule and the neighboring N atoms of the nanowire and mostly arises from the O 2p and N 2p orbitals, respectively, indicating that the spin state has a character of strong localization. However, for the CO molecules adsorbed on the $M_{12}N_{12}$-based nanowires, there is no magnetization.

The electronic band structures and density of states (DOS) were calculated for the stable configurations of the considered molecules adsorbed on the $M_{12}N_{12}$-based nanowires. All the band gaps are summarized in Table 3 and 4, and only the band structures and DOSs of the most stable configurations for each composition are shown in Fig. 7 and Fig. 8, respectively. As discussed above, the three molecules are all chemisorbed on the $M_{12}N_{12}$-based nanowires, accompanied with apparent charge transfer. Accordingly, the band structures in $M_{12}N_{12}$-based nanowires are expected to be apparently changed after the molecule adsorption. Comparing with the band structures of the pure $M_{12}N_{12}$-based nanowires, the band structures show that the band structures are modified apparently after the three molecules adsorption, indicating that the adsorption of the three molecules changes the electronic properties of the $M_{12}N_{12}$-based nanowires. Furthermore, comparing with the DOSs of the most stable structures of the pure $M_{12}N_{12}$-based nanowires, the total and partial DOS of the nanowire-molecule systems and the LDOS of the molecules show that these molecules modulate the electronic properties of the pure $M_{12}N_{12}$-based nanowires in different manners: (i) CO and NO_2 molecules adsorption introduces certain impurity states in the band gap and creation of localized states near the Fermi level, thus, these

molecules adsorption will decrease the original band gap. On the other hand, LDOS analysis shows that both of CO and NO_2 molecules adsorption will introduce fully occupied states in the valence band, and these states are nonlocalized, indicating that the interaction between these molecules and the nanowires is strong. (ii) The NO and NO_2 molecules adsorption induces unoccupied local states in the conduction band. More importantly, for the adsorption of NO molecule on the $Al_{12}N_{12}$-based nanowire, the Fermi level shifts into original conduction bands.

3.3 The potential applications of the $M_{12}N_{12}$-based nanowires for CO, NO, and NO_2 detection

If the $M_{12}N_{12}$-based nanowires are suitable for serving gas sensors for CO, NO, and NO_2 detection, the three molecules should be chemically adsorbed on the $M_{12}N_{12}$-based nanowires with apparent adsorption energy, and have sufficient charge transfer with the nanowires to influence the electrical conductivity of the $M_{12}N_{12}$-based nanowires. Our results suggest that all the three molecules can be chemically adsorbed on the nanowires with proper adsorption energies (≥ 0.4 eV), which are large enough to prevent spontaneous desorption at room temperature. Meanwhile, our results further indicate that there are apparent charge transfers ($0.05 \sim 0.512$ e, and most of the isomers are larger than 0.15 e) between the nanowires and molecule. These two factors make the $M_{12}N_{12}$-based nanowires suitable for CO, NO, and NO_2 detection. Furthermore, we can estimate the electric conductivity change of the $M_{12}N_{12}$-based nanowires before and after adsorption according to the following equation [52]

15

$$\sigma \propto \exp(\frac{-E_g}{2kT}),$$

where σ is the electric conductivity of the configurations, E_g is the band gap value of the configurations, k is the Boltzmann's constant, and T is the thermodynamic temperature. Our results suggest that the change of band gaps for the most stable configurations of CO, NO, and NO_2 molecules adsorbed on the $Al_{12}N_{12}$-based (or $Ga_{12}N_{12}$-) nanowire is in the range of 0.041 to 1.284 eV (or 0.404 to 0.795 eV) with respect to that of the corresponding nanowire. Therefore, the CO, NO, and NO_2 molecules can be detected by calculating the conductivity change of the $M_{12}N_{12}$-based nanowires before and after the adsorption process.

However, it worth noting that the strong interaction between the $M_{12}N_{12}$-based nanowires and certain molecules may also brings some serious drawbacks. That is to say, strong adsorption of a certain molecule on the $M_{12}N_{12}$-based nanowires implies that desorption of this gas molecule from the $M_{12}N_{12}$-based nanowires could be quite difficult and the devices may suffer from a longer recovery time. The recovery time τ, which relates to the adsorption energy E_{ads}, can be expressed as $\tau = v_0^{-1} e^{-E_{ads}/kT}$, where v_0 the attempt frequency, k the Boltzmann's constant, and T the temperature. Our results indicate that the adsorption energies of CO, NO, and NO_2 molecules on the $M_{12}N_{12}$-based nanowires are moderate (-0.405 to -0.796 eV), so that the recovery time of the $M_{12}N_{12}$-based nanowire sensors for CO, NO, and NO_2 at room temperature should be very short, except for the case of NO_2 molecule on the $Al_{12}N_{12}$-based nanowire. Based on the above formula, Peng *et al.* [53] predicted that the recovery

16

time of carbon nanotubes-based sensors for NO_2 at room temperature is in the range of 5 μs and 16 s for the adsorption energies of -0.34 to -0.79 eV, and the recovery time of 12 hours corresponds to adsorption energy of -1.00 eV. Therefore, the adsorption enegy (-1.157 eV) of NO_2 molecule on the $Al_{12}N_{12}$-based nanowire is too large to make the recovery time of $Al_{12}N_{12}$-based nanowire be greater than 12 hours, which precludes the applications of the $Al_{12}N_{12}$-based nanowire as NO_2 sensors. In combination with the fact that the reasonable adsorption energies, apparent charge transfer, and the change of the electric conductivity, the $Al_{12}N_{12}$-based nanowire should be good CO and NO sensors with quick response as well as short recovery time, while the $Ga_{12}N_{12}$-based nanowire should be promising gas sensors for CO, NO, and NO_2 detection.

It is well known that an ideal gas sensor also has to show selectivity in order to distinguish between different kinds of gases. Firstly, we have considered several other common gases (CO_2, H_2, N_2, and O_2) adsorbed on the $M_{12}N_{12}$-based nanowires. The most stable configurations of these gas molecules adsorbed on the $M_{12}N_{12}$-based nanowires are shown in Fig. 9, and the related results are summarized in Table 5. It is found that the CO_2, H_2 and N_2 molecules are adsorbed weakly on the $M_{12}N_{12}$-based nanowires. The O_2 molecule can be chemically adsorbed on the $Al_{12}N_{12}$-based nanowire with the adsorption energy of -0.456 eV, however, it can weakly adsorb on the $Ga_{12}N_{12}$-based nanowire with adsorption energy of 0.197 eV, indicating the high inertness of the $Ga_{12}N_{12}$-based nanowire toward O_2 molecule in ambient conditions. The charge transfer between CO_2, H_2 and N_2 molecules and nanowires are much

17

smaller than that of CO, NO, and NO_2 molecules adsorbed on the $M_{12}N_{12}$-based

nanowires. More importantly, the band gap energies of the $M_{12}N_{12}$-based nanowires

are hardly changed by the adsorption of these molecules. These results indicate that

the magnitudes of conductivity changes for the CO, NO, and NO_2 molecules are

larger than those of CO_2, H_2 and N_2. Although the chemical adsorption of O_2 on the

$Al_{12}N_{12}$-based nanowire leads to apparent charge transfer between the $Al_{12}N_{12}$-based

nanowire and O_2 molecule and the change of E_g, according to the equation of

$\sigma \propto \exp(\dfrac{-E_g}{2kT})$, the change of the electric conductivity is very different from those of

the adsorption of CO, NO, and NO_2. Furthermore, the change of the electric

conductivity is different for the different molecule (CO, NO, and NO_2) adsorption,

indicating that it can be differentiate a certain gas in the presence of other gases via

comparing the change of the electric conductivity. Hence, it can be deduced that the

$M_{12}N_{12}$-based nanowires selectively act as gas sensor device between the molecules

including CO, NO, NO_2, CO_2, H_2, N_2, and O_2.

4. Conclusions

In conclusion, using density functional theory calculations, the structural and

electronic properties and the applications as gas sensors of cluster-assembled

nanowires based on $M_{12}N_{12}$ (M=Al and Ga) clusters have been investigated. We begin

the investigation by predicting that the novel MN nanowires can be produced via the

coalescence of stable $M_{12}N_{12}$ fullerene-like clusters. The $M_{12}N_{12}$-based nanowires

have semiconducting electrical properties with direct energy gaps, and are particularly

stable at room temperature for long enough to allow for their characterization and applications.

Then, the interaction between the $M_{12}N_{12}$-based nanowires and CO, NO, and NO_2 molecules is studied in order to find novel gas sensors for CO, NO, and NO_2 detection. Our results show that the three molecules are chemisorbed on the $M_{12}N_{12}$-based nanowires with reasonable adsorption energies and apparent charge transfer. The electronic properties of the $M_{12}N_{12}$-based nanowires present dramatic changes after the adsorption of the CO, NO, and NO_2 molecules, especially their electric conductivity. However, the very strong adsorption of NO_2 on the $Al_{12}N_{12}$-based nanowire makes desorption difficult, which precludes its applications to NO_2 sensors. In addition to the adsorption of NO_2 on the $Al_{12}N_{12}$-based nanowire, due to the reasonable adsorption energies, apparent charge transfer, the change of the electric conductivity, and the short recovery time, the $Al_{12}N_{12}$-based nanowire should be good CO and NO sensors with quick response as well as short recovery time, while the $Ga_{12}N_{12}$-based nanowire should be promising gas sensors for CO, NO, and NO_2 detection.

References

[1] X. Huang and Y. Choi, Sensor. Actuat. B-Chem., 2007, **122**, 659–671.

[2] X, Liu, S. Cheng, H. Liu, S. Hu, D. Zhang and H. Ning, Sensors, 2012, **12**, 9635–9665.

[3] S. Chiu and K. Tang, Sensors, 2013, **13**, 14214–14247.

[4] Y. Liu, J. Parisi, X. Sun and Y. Lei, J. Mater. Chem. A, 2014, **2**, 9919–9943.

[5] R. Yan, D. Gargas and P. Yang, Nat. Photonics, 2009, **3**, 569–576.

[6] N. S. Ramgir, Y. Yang and M. Zacharias, Small, 2010, **6**, 1705–1722.

[7] M. M. Arafat, B. Dinan, S. A. Akbar and A. S. M. A. Haseeb, Sensors, 2012, **12**, 7207–7258.

[8] J. Huang and Q. Wan, Sensors, 2009, **9**, 9903–9924.

[9] P. T. Hernandez, A. J. T. Naik, E. J. Newton, Stephen M. V. Hailesc and I. P. Parkin, J. Mater. Chem. A, 2014, **2**, 8952–8960.

[10] S. Zhao, H. P. T. Nguyen, M. G. Kibria and Z. Mi, Prog. Quant. Electron., 2015, **44**, 14–68.

[11] Y. Zhang, J. Wu, M. Aagesen and H. Liu, J. Phys. D: Appl. Phys., 2015, **48**, 463001.

[12] N. P. Dasgupta, J. Sun, C. Liu, S. Brittman, S. C. Andrews, J. Lim, H. Gao, R. Yan and P. Yang, Adv. Mater., 2014, **26**, 2137–2184.

[13] M. G. Kibria and Z. Mi, J. Mater. Chem. A, 2016, **4**, 2801–2820.

[14] J. Wallys, J. Teubert, F. Furtmayr, D. M. Hofmann and M. Eickhoff, Nano Lett., 2012, **12**, 6180−6186.

[15] J. K. Hyun, S. Zhang and L. J. Lauhon, Annu. Rev. Mater. Res., 2013, **43**, 451−479.

[16] S. Chattopadhyay, A. Ganguly, K. Chen and L. Chen, Crit. Rev. Solid State, 2009, **34**, 224–279.

[17] S. J. Pearton, F. Ren, Y. Wang, B. H. Chu, K. H. Chen, C. Y. Chang, W. Lim, J. Lin and D. P. Norton, Prog. Mater. Sci., 2010, **55**, 1–59.

[18] S. N. Khanna and P. Jena, Phys. Rev. Lett., 1992, **69**, 1664.

[19] S. M. Woodley and C. R. A. Catlow, Nat. Mater., 2008, **7**, 937–946 .

[20] A. W. Castleman Jr. and S. N. Khanna, J. Phys. Chem. C, 2009, **113**, 2664–2675.

[21] M. Qian, A. C. Reber, A. Ugrinov, N. K. Chaki, S. Mandal, H. M. Saavedra, S. N. Khanna, A. Sen and P. S. Weiss, ACS Nano, 2010, **4**, 235–240.

[22] S. A. Claridge, A. W. Castleman Jr., S. N. Khanna, C. B. Murray, A. Sen and P. S. Weiss, ACS Nano, 2009, **3**, 244–255.

[23] P. Jena, J. Phys. Chem. Lett., 2013, **4**, 1432–1442.

[24] Y. Yong, B. Song and P. He, Phys. Chem. Chem. Phys., 2011, **13**, 16182–16189.

[25] J. Li, Y. Xia, M. Zhao, X. Liu, C. Song, L. Li, F. Li and B. Huang, J. Phys.: Condens. Matter, 2007, 19, 346228.

[26] Z. Liu, X. Wang, G. Liu, P. Zhou, J. Sui, X. Wang, H. Zhu and Z. Hou. Phys. Chem. Chem. Phys., 2013, **15**, 8186–8198.

[27] J. M. Matxain, L. A. Eriksson, J. M. Mercero, X. Lopez, M. Piris, J. M. Ugalde, J. Poater, E. Matito and M. Solà, J. Phys. Chem. C, 2007, **111**, 13354–13360.

[28] V. V. Pokropivny, A. S. Smolyar and A. V. Pokropivny, Phys. Solid State, 2007, **49**, 591–598.

[29] Y. Yong, K. Liu, B. Song, P. He, P. Wang and H. Li, Phys. Lett. A, 2012, **376**,

1465–1467.

[30] J. L. Li, T. He and G. W. Yang, Nanoscale, 2012, **4**, 1665–1670.

[31] A. Soltani, S. G. Raz, M. R. Taghartapeh, A. V. Moradi and R. Z. Mehrabian, Comput. Mater. Sci., 2013, **79**, 795–803.

[32] J. Beheshtian, A. A. Peyghan and Z. Bagheri, Comput. Mater. Sci., 2012, **62**, 71–74.

[33] M. T. Baei, A. Soltani, S. Hashemian and H. Mohammadian, Can. J. Chem., 2014, **92**, 605–610.

[34] M. T. Baei, A. Soltani, P. Torabi and S. Hashemian, Monatsh. Chem., 2015, **146**, 891–896.

[35] M. T. Baei, Comput. Theo. Chem., 2013, **1024**, 28–33.

[36] J. Beheshtian, M. Kamfiroozi, Z. Bagheri and A. A. Peyghan, Chin. J. Chem. Phys., 2012, **25**, 60–64.

[37]A. A. Peyghan and H. Soleymanabad, Curr. Sci., 2015, **108**, 1910–1914.

[38] B. Delley, J. Chem. Phys., 1990, **92**, 508–517.

[39] B. Delley, J. Chem. Phys. , 2000, **113**, 7756–7764.

[40] J. P. Perdew, K. Burke and M. Ernzerhof, Phys. Rev. Lett., 1996, **77**, 3865–3868.

[41] H. J. Monkhorst and J. D. Pack, Phys. Rev. B., 1976, **13**, 5188–5192.

[42] Y. Yong, B. Song and Pimo He, J. Phys. Chem. C, 2011, **115**, 6455–6461.

[43] Z. Liu, X. Wang, J. Cai, G. Liu, P. Zhou, K. Wang and H. Zhu, J. Phys. Chem. C, 2013, **117**, 17633–17643.

[44] Y. Yong, X. Li, X. Hao, J. Cao and T. Li, RSC Adv., 2014, **4**, 37333–37341.

[45] D. J. Carter, J. D. Gale, B. Delley and C. Stampfl, Phys. Rev. B, 2008, **77**, 115349.

[46] M. Zhao, Y. Xia, X. Liu, Z. Tan, B. Huang, C. Song and L. Mei, J. Phys. Chem. B, 2006, **110**, 8764–8768.

[47] Y. Yong, C. Li, X. Li, T. Li, H. Cui and S. Lv, J. Phys. Chem. C, 2015, **119**, 7534−7540.

[48] Y. Yong, X. Li, T. Li, H. Cui and S. Lv, Europhys. Lett., 2015, **111**, 10006.

[49] R. Q. Wu, M. Yang, Y. H. Lu, Y. P. Feng, Z. G. Huang and Q. Y. Wu, J. Phys. Chem. C, 2008, 112, 15985–15988.

[50] E. R. Davidson and S. A. Chakravorty, Theor. Chim. Acta, 1992, **83**, 319–330.

[51] Z. Zanolli and J. C. Charlier, ACS Nano, 2012, **6**, 10786–10791.

[52] S. S. Li, Semiconductor Physical Electronics, 2nd ed. Springer: USA, 2006.

[53] S. Peng, K. Cho, P. Qi and H. Dai, Chem. Phys. Lett., 2004, 387, 271–276.

Table 1. The calculated binding energy per MN (E_b), dimerization energy (E_d), and HOMO-LUMO gap (E_g) for the $M_{12}N_{12}$ (M=Al and Ga) monomers and the three lowest-energy structures (shown in Fig. 1(A, B, C)) of $M_{12}N_{12}$ dimers.

System[a]	E_b (eV)	E_d (eV)	E_g (eV)
$Al_{12}N_{12}$	9.437	--	2.706
Al-A	9.8041	8.814	2.834
Al-B	9.8035	8.798	2.836
Al-C	9.670	6.303	2.662
$Ga_{12}N_{12}$	7.150	--	2.046
Ga-A	7.438	6.988	2.201
Ga-B	7.437	6.969	1.751
Ga-C	7.372	5.412	2.034

[a] The isomers of $Al_{12}N_{12}$ ($Ga_{12}N_{12}$) dimers are labeled as Al-A, Al-B, and Al-C (Ga-A, Ga-B, and Ga-C), respectively.

Table 2. The calculated binding energy per MN (E_b), the length of translational

periodicity (L), and band gap (E_g) for the three the $M_{12}N_{12}$-based nanowires (I-III).

Nanowire	E_b (eV)	L (Å)	E_g (eV)
Al-I	10.167	13.096	2.004
Al-II	10.166	13.093	2.027
Al-III	9.955	14.679	1.674
Ga-I	7.750	13.480	1.200
Ga-II	7.747	13.484	1.137
Ga-III	7.622	15.130	0.925

Table 3. Calculated adsorption energy (E_{ads}), band energy gap (E_g), and charge

transfer from the nanowire to molecule (E_T), and total magnetic moment (μ_T) for the

CO, NO, and NO_2 molecule adsorption on the $Al_{12}N_{12}$-based nanowire.

System [a]	E_{ads} (eV)	E_g (eV)	E_T (e)	μ_T (μ_B)
Al-CO-1	-0.584	2.045	0.193	0
Al-CO-2	-0.270	1.236	-0.242	0
Al-NO-1	-0.720	0.174	-0.305	1.0
Al-NO-2	-0.648	0.920	0.050	1.0
Al-NO_2-1	-1.157	0.879	-0.512	1.0
Al-NO_2-2	-0.995	0.649	-0.116	1.0

Table 4. Calculated adsorption energy (E_{ads}), band energy gap (E_g), and charge transfer from the nanowire to molecule (E_T), and total magnetic moment (μ_T) for the CO, NO, and NO$_2$ molecule adsorption on the Ga$_{12}$N$_{12}$-based nanowire.

System [a]	E_{ads} (eV)	E_g (eV)	E_T (e)	μ_T (μ_B)
Ga-CO-1	-0.796	1.035	-0.213	0
Ga-CO-2	-0.457	1.293	-0.185	0
Ga-CO-3	-0.327	1.271	0.167	1.0
Ga-NO-1	-0.405	0.583	0.053	1.0
Ga-NO$_2$-1	-0.675	0.535	-0.140	1.0
Ga-NO$_2$-2	-0.399	0.164	-0.171	1.0
Ga-NO$_2$-3	-0.210	0.251	-0.320	1.0

Table 5. Calculated adsorption energy (E_{ads}), band energy gap (E_g), and charge transfer from the nanowire to molecule (E_T) for the CO_2, H_2, N_2, and O_2 molecule adsorption on the $M_{12}N_{12}$-based nanowires.

System	E_{ads} (eV)	E_g (eV)	E_T (e)
Al-CO$_2$	-0.247	2.014	0.054
Al-H$_2$	-0.105	2.018	0.081
Al-N$_2$	-0.036	0.055	2.007
Al-O$_2$	-0.456	-0.333	2.105
Ga-CO$_2$	-0.144	0.082	1.208
Ga-H$_2$	-0.077	0.010	1.201
Ga-N$_2$	-0.064	0.080	1.212
Ga-O$_2$	0.197	-0.039	1.200
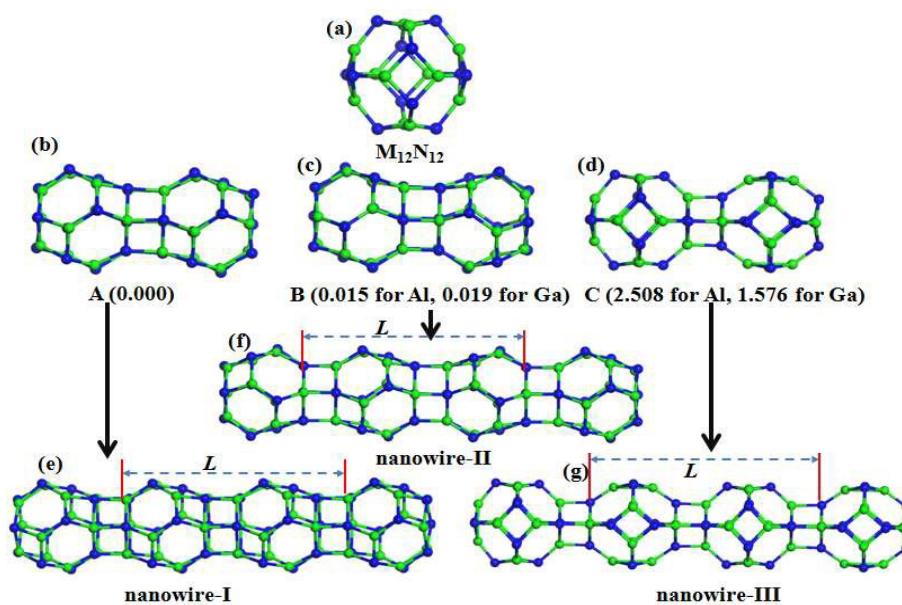
Fig. 1. The optimized configurations of the $M_{12}N_{12}$-based (M=Al and Ga) nanostructures: (a) the fullerene-like $M_{12}N_{12}$ clusters; (b-d), the three lowest-energy structures of $M_{12}N_{12}$ dimers; (e-g) the $M_{12}N_{12}$-based nanowires (I-III) assembled by $M_{12}N_{12}$ clusters. The green balls represent Al or Ga atoms, and blue balls represent N atoms. Values in parentheses (in eV) are relative energies with respect to the structure A for each composition. "*L*" as shown in figures is the length of translational periodicity for the optimized nanowires.
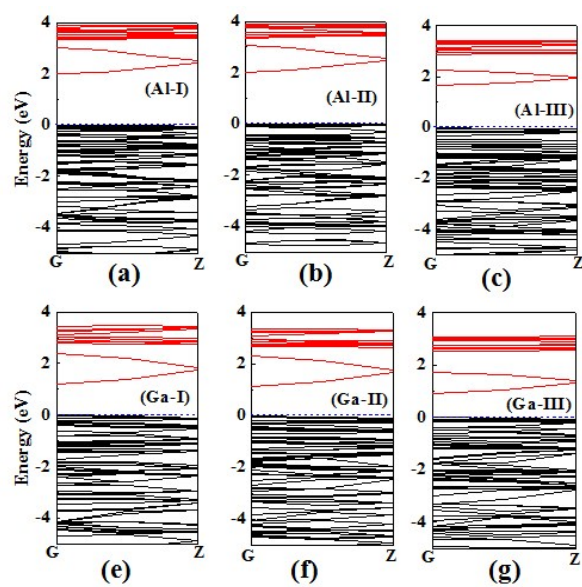
Fig. 2. The band structures of the $M_{12}N_{12}$-based nanowires. Fermi-level energy is set

to zero and marked by blue dotted lines. Red lines: unoccupied; black lines: occupied.
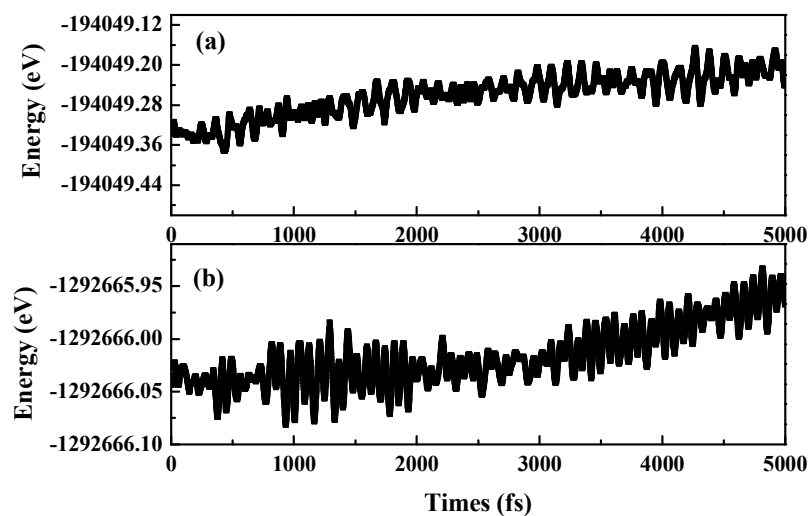
Fig. 3. Variation in the energy (eV) of the most stable configuration of the (a) $Al_{12}N_{12}$-based and (b) $Ga_{12}N_{12}$-based nanowire as a function of time at T=300 K.
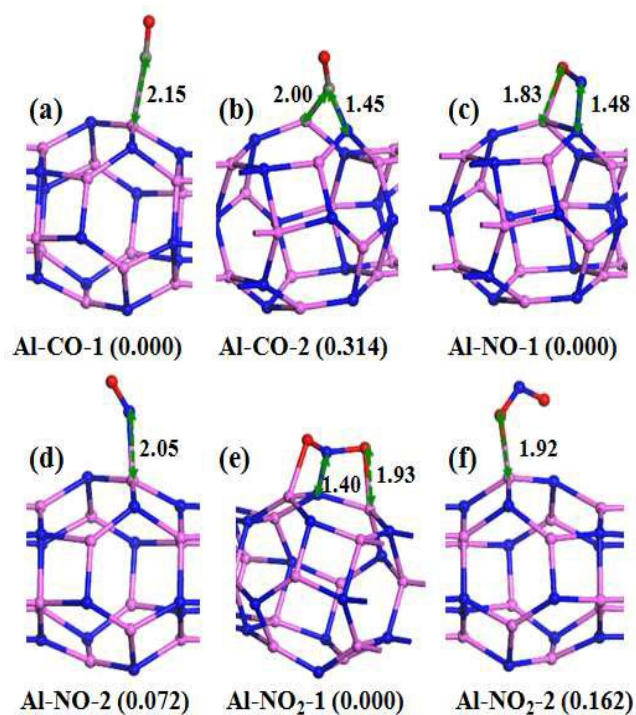
Fig. 4. Optimized structures of $Al_{12}N_{12}$-based nanowire with gas molecule adsorption: (a) and (b) CO; (c) and (d) NO; (e) and (f) NO_2. We only show the structure around the adsorbed molecule. Values in parentheses are relative energies with respect to the most stable isomer for each adsorption in eV. The bond lengths (in Å) between the molecule and the nanowire are also given. Al, N, C and O atoms are pink, blue, grey and red, respectively.
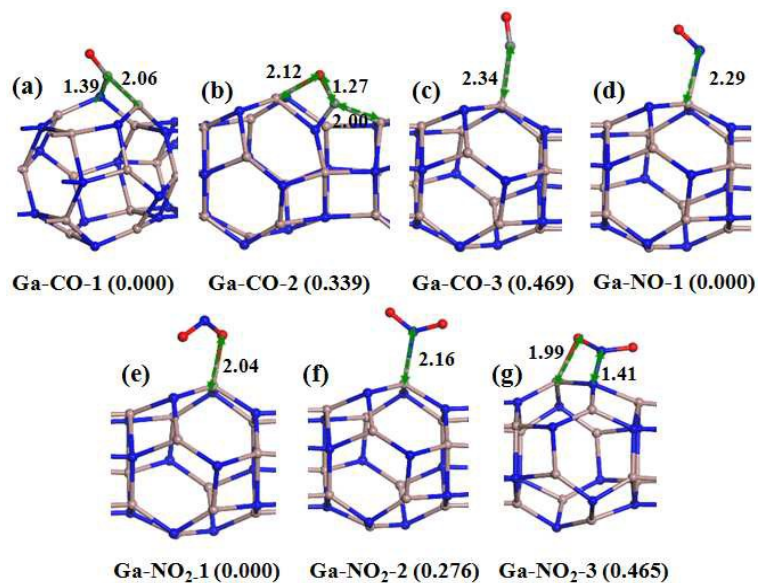
Fig. 5. Optimized structures of $Ga_{12}N_{12}$-based nanowire with gas molecule adsorption: (a), (b) and (c) CO; (d) NO; (e), (f) and (g) NO_2. We only show the structure around the adsorbed molecule. Values in parentheses are relative energies with respect to the most stable isomer for each adsorption in eV. The bond lengths (in Å) between the molecule and the nanowire are also given. Ga, N, C and O atoms are brown, blue, grey and red, respectively.
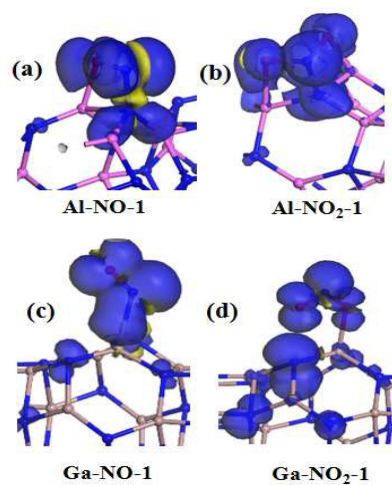
Fig. 6. Spin density of the most stable configurations of NO and NO_2 adsorption on the $M_{12}N_{12}$-based nanowires with isovalues of ± 0.005 e/$\mathring{A}^3$.
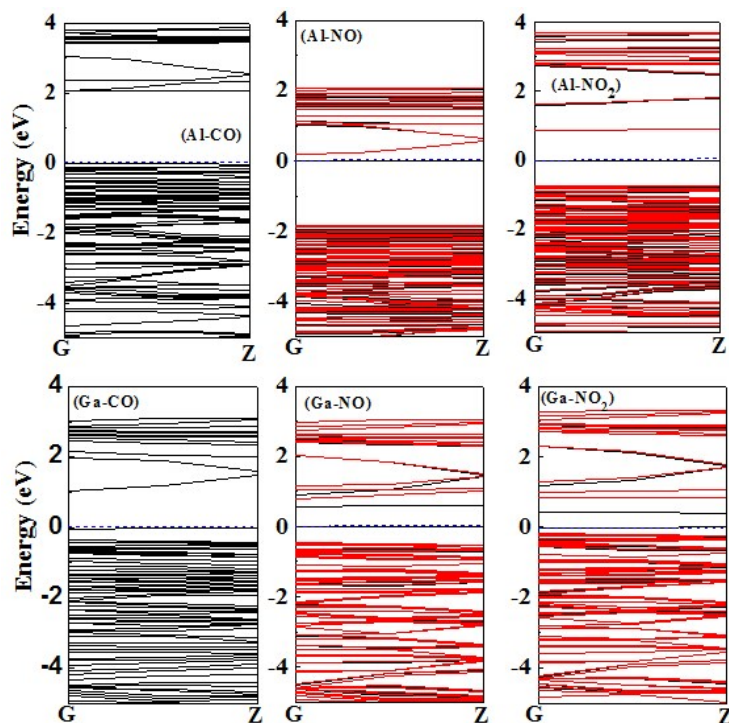
Fig. 7. The band structures of the most stable configurations of CO, NO, and NO$_2$ adsorption on the M$_{12}$N$_{12}$-based nanowires. Fermi-level energy is set to zero and marked by blue dotted lines. The black and red lines are for majority spin and minority spin, respectively.
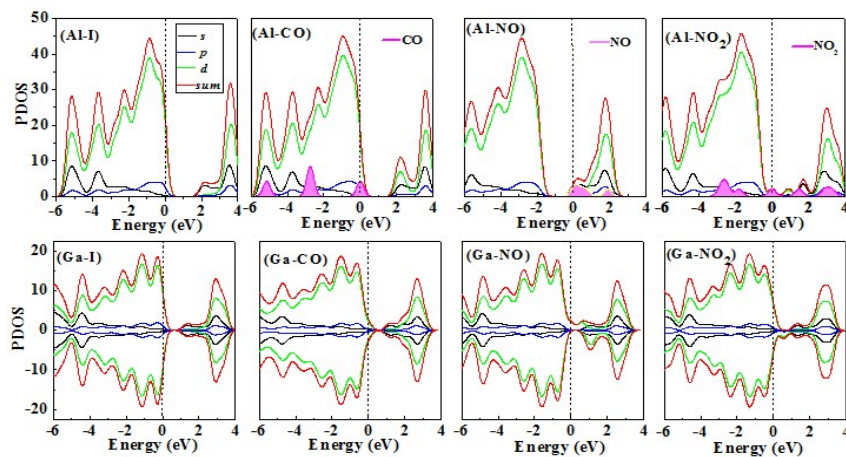
Fig. 8. Total and partial density of states (DOS) of the most stable configurations of the pure $M_{12}N_{12}$-based nanowires (Al-I and Ga-I) and their adsorption systems with CO, NO, and NO_2. The LDOS of gas molecules is also plotted (magenta filled area under DOS curve). The vertical dashed line is the Fermi-level energy. The positive and negative values represent spin-up and spin-down states, respectively.
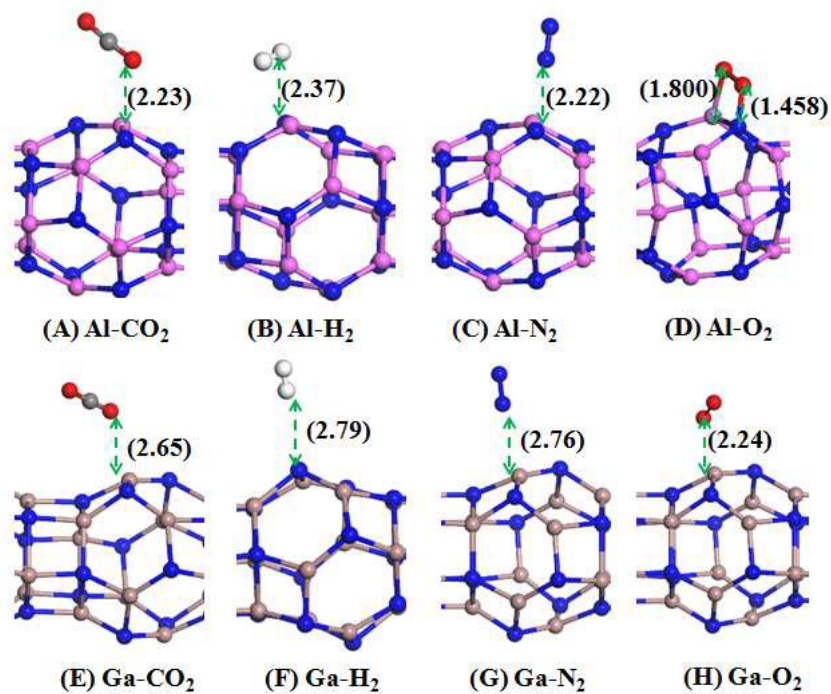
Fig. 9. The most stable structures of the $M_{12}N_{12}$-based nanowires with gas molecule adsorption: (A) CO_2, (B) H_2, (C) N_2 and (D) O_2 adsorbed on the $Al_{12}N_{12}$-based nanowire, (E) CO_2, (F) H_2, (G) N_2 and (H) O_2 adsorbed on the $Ga_{12}N_{12}$-based nanowire, respectively. We only show the structure around the adsorbed molecule. The shortest distance (in Å) between the molecule and the nanowire are also given.